

## Full Paper

# Genome-wide profiling of *Sus scrofa* circular RNAs across nine organs and three developmental stages

Guoming Liang<sup>1,2,3</sup>, Yalan Yang<sup>1,2,3</sup>, Guanglin Niu<sup>1</sup>, Zhonglin Tang<sup>1,2,3,\*</sup>, and Kui Li<sup>1,2,\*</sup>

<sup>1</sup>State Key Laboratory of Animal Nutrition, Institute of Animal Science, Chinese Academy of Agricultural Sciences, Beijing 100193, China, <sup>2</sup>Department of Pig Genomic Design and Breeding, Agricultural Genome Institute at Shenzhen, Chinese Academy of Agricultural Sciences, Shenzhen 518124, China and <sup>3</sup>Shenzhen Key Laboratory of Phenotype Analysis and Utilization of Agricultural Genome, Agricultural Genome Institute at Shenzhen, Chinese Academy of Agricultural Sciences, Shenzhen 518124, China

\*To whom correspondence should be addressed. Tel. +86 10 6281 8180. Fax. +86 10 6281 8180.

Email: zhonglinqy\_99@sina.com (Z.T.); likui@caas.cn (K.L.)

Edited by Dr. Minoru Ko

Received 28 October 2016; Editorial decision 29 April 2017; Accepted 3 May 2017

## Abstract

The spatio-temporal expression patterns of Circular RNA (circRNA) across organs and developmental stages are critical for its function and evolution analysis. However, they remain largely unclear in mammals. Here, we comprehensively analysed circRNAs in nine organs and three skeletal muscles of Guizhou miniature pig (*S. scrofa*), a widely used biomedical model animal. We identified 5,934 circRNAs and analysed their molecular properties, sequence conservation, spatio-temporal expression pattern, potential function, and interaction with miRNAs. *S. scrofa* circRNAs show modest sequence conservation with human and mouse circRNAs, are flanked by long introns, exhibit low abundance, and are expressed dynamically in a spatio-temporally specific manner. *S. scrofa* circRNAs show the greatest abundance and complexity in the testis. Notably, 31% of circRNAs harbour well-conserved canonical miRNA seed matches, suggesting that some circRNAs act as miRNAs sponges. We identified 149 circRNAs potentially associated with muscle growth and found that their host genes were significantly involved in muscle development, contraction, chromatin modification, cation homeostasis, and ATP hydrolysis-coupled proton transport; moreover, this set of genes was markedly enriched in genes involved in tight junctions and the calcium signalling pathway. Finally, we constructed the first public *S. scrofa* circRNA database, allowing researchers to query comprehensive annotation, expression, and regulatory networks of circRNAs.

**Key words:** circRNAs, pig, profiling, organs, skeletal muscle

## 1. Introduction

Circular RNAs (circRNAs) were generally believed to be linear until their circular form was observed via electron microscopy in 1979.<sup>1</sup>

CircRNA is formed by exon-scrambling, in which a splice donor is spliced to an upstream acceptor rather than a downstream acceptor during transcription. While exons are most common, some introns

can also form circRNAs during transcription. Usually, circRNAs are expressed at a relatively low level. CircRNAs have been identified in large numbers by deep RNA sequencing and are believed to be widely expressed in eukaryotic cells.<sup>2–6</sup> Most circRNA is flanked by GT/AG splice sites reflecting back-splicing. CircRNA back-splicing locations are in nearly the same locations in orthologous genes and exons in animals, showing that circRNAs are conserved in animals<sup>4,7</sup> and plants.<sup>6</sup> Although many circRNAs have been discovered in mouse and human, little is known about circRNAs in other mammals.

CircRNA expression is spatio-temporally regulated in *Drosophila* brains,<sup>7</sup> pig brains,<sup>8</sup> and mouse pre-implantation embryos.<sup>5</sup> CircRNAs also show tissue-specific expression in the heart and lung during human fetal development.<sup>9</sup> It is believed that circRNAs bind miRNAs and thus regulate gene expression at the post-transcriptional level. For example, *CDRIas* functions as an efficient miRNA sponge, binding miR-7 and allowing mRNAs to escape degradation following miRNA binding.<sup>2,10</sup> *Sry* can form a circRNA that is also proposed to act as a miRNA sponge.<sup>10</sup> In addition to regulating mRNA translocation by acting as a miRNA sponge, circRNA can also regulate transcription through specific RNA–RNA interactions. A recently described subclass of circRNAs, ElciRNAs, contains introns among exons after RNA circling. In human cells, some ElciRNAs associate with RNA polymerase II, thus interacting with U1 snRNP and enhancing parental gene expression in *cis*.<sup>11</sup> The functions of circRNAs remain largely unclear. Investigating the spatio-temporal distribution of circRNAs is critical to understanding their biological functions. However, little is known about the expression patterns of circRNAs across organs and developmental stages in mammals.

The domestic pig (*Sus scrofa*) has had a close and complex relationship with humans for at least 10,000 years.<sup>12–14</sup> The pig is an important domesticated farm animal that provides protein for humans, as well as a non-rodent animal model used in biomedical research. In comparison with traditional rodent models, the pig is more similar to humans in body size, growth, development, immunity, physiology, and metabolism, as well as genomic sequence.<sup>15–17</sup> Recent studies of the *S. scrofa* genome and transcriptome have increased the utility of this species as a biomedical model.<sup>14,18–21</sup> However, in comparison with mice and humans, knowledge regarding the pig transcriptome across organs and developmental stages is very limited.<sup>22–25</sup> Thousands of circRNAs have been discovered in fetal pig brains;<sup>8</sup> however, the identities and expression profiles of *S. scrofa* circRNAs remain largely uncharacterized.

We performed genome-wide analysis of circRNA across nine organs (heart, liver, spleen, lung, kidney, ovary, testis, muscle, and fat) and three skeletal muscles at multiple developmental stages (0, 30, and 240 days after birth) from Guizhou miniature pigs (a native Chinese pig in the Guizhou province), which are widely used as an animal model in biomedical research. We systematically identified *S. scrofa* circRNAs and analysed their molecular properties, sequence conservation, spatio-temporal expression patterns, potential functions, and binding sites for miRNAs. Finally, we constructed the first public *S. scrofa* circRNA database.

## 2. Materials and methods

Nine organs, including the heart, liver, spleen, lung, kidney, ovary, testis, skeletal muscle, and fat, were collected from three male and female Guizhou miniature pigs at postnatal day 240. We also collected longissimus muscle samples from three Guizhou miniature

pigs at postnatal days 0 and 30. Total RNA was isolated from each sample by TRIZOL reagent according to the manufacturer's protocols, after which total RNA was pooled by tissue type and age for RNA-seq analysis. Total RNA was reverse-transcribed according to the manufacturer's instructions. Paired-end reads 100 bp in length were sequenced by an Illumina HiSeq 2500. RNA-seq data were deposited in the Gene Expression Omnibus (accession codes GSE73763).

Reads were first mapped to the pig genome by Bowtie2,<sup>26</sup> after which the mapped reads were filtered out by SAMtools.<sup>27</sup> For the unmapped reads, 20 mers were cut off from both ends of each paired-end read, after which the remaining 60 mers were aligned to the pig genome in reverse orientation by Bowtie2.<sup>26</sup> We used the `find_circ` package<sup>2,4</sup> to identify circRNA. The workflow is shown in Supplementary Fig. S5.

In this study, a circRNA was designated as conserved when it was produced from orthologous genes in different species. We extracted pig-to-human and pig-to-mouse orthologous gene tables from BioMart ([www.biomart.org](http://www.biomart.org)). Human and mouse circRNAs were identified by a previous study.<sup>4,28</sup>

CircRNA expression was quantified by calculating the number of junction spanning reads per million reads of each sample. Junction spanning reads that were less than 5 reads supported were excluded when determining circRNA expression levels. Differentially expressed circRNAs were identified by the chi-square test with  $P \leq 0.05$  and had fold-change  $\geq 2$  (or  $\leq 0.5$ ) between any two tissues samples.

Four-hundred and eleven mature pig miRNA sequences were obtained from miRBase.<sup>29</sup> We used microtar,<sup>30</sup> Miranda,<sup>31</sup> and RNAhybrid<sup>32</sup> to identify circRNA binding sites for miRNAs. To decrease the proportion of false-positive results, intersections predicted by all three programs were treated as the final set of target miRNAs.

The circRNA database is composed of a web interface and a SQLite database engine, which is used to store and manage all data. The data processing programs are written in Python (version 3.4.4). The web interface is built by Django (version 1.8.13) a Python Web framework. Google<sup>®</sup> charts (<https://developers.google.com/chart/>) and D3.js (<https://d3js.org/>) were used for interface development. The circRNA database is coded as a Django project and is deployed by uWSGI (<https://uwsgi-docs.readthedocs.io>). Web services were built using nginx (version 2.10.0), an HTTP and reverse proxy server.

## 3. Results

### 3.1. Identification and characteristics of *S. scrofa* circRNAs

To perform comprehensive profiling of circular RNA in pigs, we carried out total RNA sequencing in nine adult organs (including fat, heart, kidney, liver, lung, spleen, testis, ovary, and skeletal muscle) and three skeletal muscles at 0, 30, and 240 days after birth. In this study, the identified circRNAs were flanked by GT/AG splice sites and had unambiguous break points. The genomic distance between two splice sites was less than 100 kb, and each circRNA was supported by at least 2 reads in each sample. We identified 5,934 unique circRNAs in all assessed biological tissues (Supplementary Table S1).

The analysis of chromosome distribution showed that circRNAs are widely and unevenly transcribed from *S. scrofa* chromosomes (SSCs). More circRNAs were generated from SSC1 and SSC6 in comparison with the other SSCs. Only three circRNAs were detected

on SSC-Y (Fig. 1A). The number of circRNAs was not significantly related to chromosome length or the number of genes contained in each chromosome (Supplementary Fig. S1). Most circRNAs contain multiple exons, and some circRNAs also retain introns, as indicated in a previous study.<sup>33</sup> According to the pig genes and splice junction annotations in the Ensembl database (release 78, [ftp://ftp.ensembl.org/pub/release-78/gtf/sus\\_scrofa](ftp://ftp.ensembl.org/pub/release-78/gtf/sus_scrofa)), we found that most circularizing events typically encompass less than 5 exons (average exons = 4.8). More than 90% of circRNAs are formed by multiple exons, while only 9.9% are formed by a single exon (Fig. 1B). This finding is in agreement with observations in mice.<sup>5</sup>

CircRNAs are mostly comprised of coding sequence (CDS, 68.40%) and intergenic regions (21.93%), whereas a smaller fraction (10%) also contain 5'-untranslated regions (UTRs), 3'-UTRs, or both UTRs (Fig. 1C), in agreement with a previous report.<sup>4</sup> The distribution of circRNA exonic sequence lengths resembles that of human circRNA, with a median length of 509 nucleotides, whereas that of human circRNA is 547 nucleotides.<sup>4</sup> Most *S. scrofa* circRNAs are shorter than 2 kb (4,243/5,934 = 71.5%), similar to mouse circRNAs.<sup>5</sup> The GC content of *S. scrofa* circRNA is similar to that of other small RNAs, with an average GC content of 42.67% (Fig. 1D).

### 3.2. Sequence conservation among pig, human, and mouse circRNAs

Several studies suggest that some circRNAs are evolutionarily conserved among humans and mice.<sup>4,34-36</sup> Indeed, 81 of 1,903 mouse circRNAs were mapped to human circRNAs in a report by Memczak.<sup>2</sup> Using the liftOver tool, another study found that 28.5% of mouse circRNAs are conserved in humans, while 33.3% of these circRNAs

have no human homolog.<sup>35</sup> To investigate circRNA sequence conservation between pigs and other mammals, we compared pig circRNAs to human and mouse circRNAs with clear one-to-one orthologs (<http://asia.ensembl.org/biomart/martview/>). We found that 20.20% of pig circRNAs have human orthologs, whereas 16.96% of pig circRNAs have mouse orthologs (Fig. 2A). These observations are comparable with previous reports.

To assess whether pig and human circRNAs arise from orthologous exons, we used whole-genome alignments to identify regions of the human genome that correspond to pig circRNAs and quantified the degree to which pig circRNAs overlapped with these regions. We found that 29.4% of pig circRNAs have orthologous exons in humans. In mice, 28.6% of circRNAs overlap with human circRNAs.<sup>35</sup> Blast analysis suggested that 1,510 (1510/5934 = 25.45%) and 5,189 (5189/5934 = 87.44%) *S. scrofa* circRNAs have orthologs in mice and humans, respectively (Supplementary Tables S2 and S3). These findings indicate that pig, human, and mouse circRNAs are modestly conserved and often generated from orthologous genes. Moreover, our sequence conservation analysis suggests that circRNA might have conserved functions in pigs, mice, and humans.

### 3.3. *S. scrofa* circRNAs are flanked by long introns

The sequence conservation of circRNAs among species indicated that their mechanisms of biogenesis might also be conserved. Previous studies suggested that most circRNAs are derived from exons with long flanking introns, which usually contain reverse complementary matches (RCMs) that facilitate back-splicing of the enclosed circRNAs.<sup>7,37-39</sup> To determine whether introns flank pig circRNAs, we analysed 5kb sequences length of both 5' upstream and 3' downstream sequences

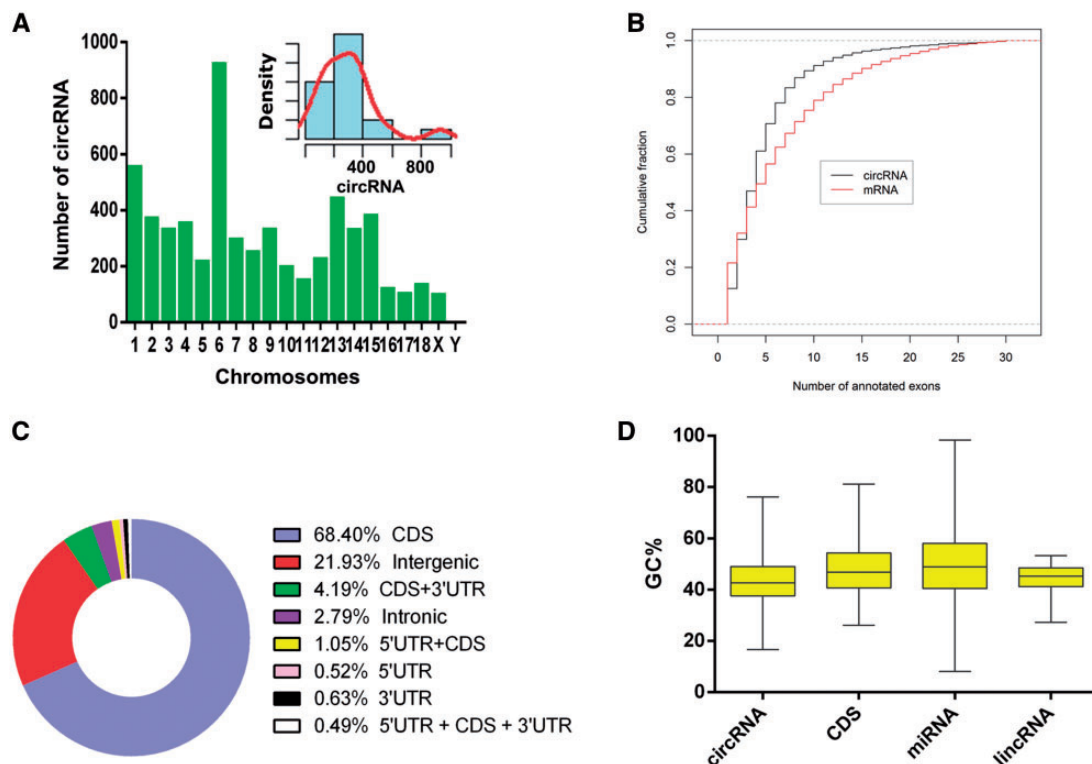


**Figure 1.** Identification and feature of circRNAs in pigs. (A) Chromosome distribution of circRNAs, the curve line represents the density of circRNAs along chromosome. (B) Distribution of exon number for circRNAs and mRNA. (C) Genomic location of circRNAs. (D) GC contents of circRNAs comparing with mRNA, miRNA and lincRNA.

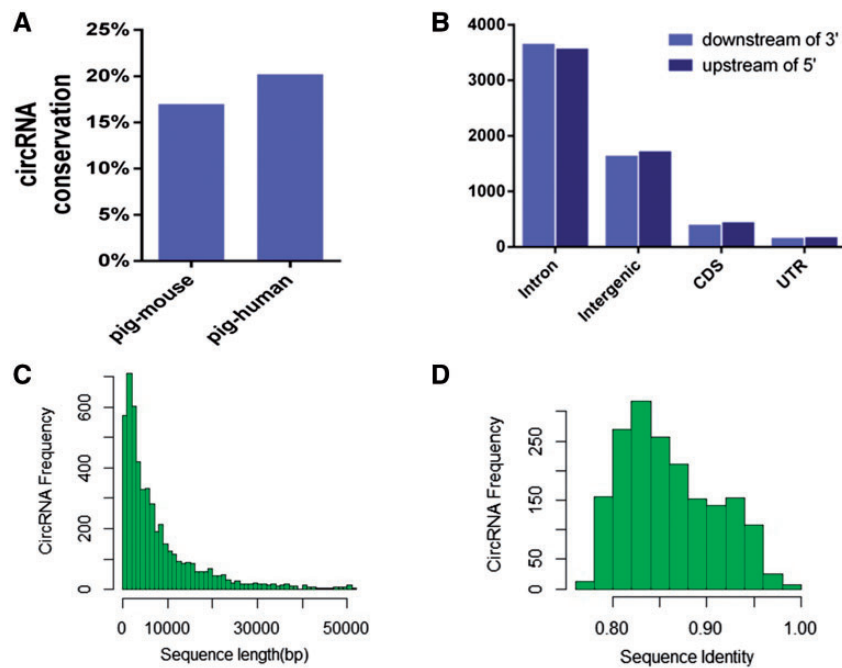


**Figure 2.** Molecular characteristics of *S. scrofa* circRNA. **(A)** Sequence conservation of *S. scrofa* circRNA compared with human and mouse ones, respectively. The percentage means that if there is a circRNA in pig, there is also an ortholog circRNA in human or mouse. **(B)** Sequences identity of flanking introns of a circRNA 5' end upstream and a 3' end downstream. **(C)** Distribution of flanking intron sequences lengths for circRNA. **(D)** Distribution of sequences identity of each intron pair that flanked circRNA.

flanking pig circRNAs. We observed that the majority of circularized exons are flanked by upstream and downstream introns. We found that 60.4% of 5' sequences upstream of circRNAs contain introns, whereas 62.4% of 3' sequences downstream of circRNAs contain introns. Moreover, 29.1 and 28.0% of the assessed regions upstream and downstream of circRNAs are intergenic regions. Few sequences flanking circRNAs are CDS, 5'-UTRs, or 3'-UTRs (Fig. 2B). We found that 2,641 circRNAs are flanked by intron sequences on the 5' and 3' ends. The median length of the flanking introns on both sides of the identified circRNAs is 5,040 bp (Fig. 2C). Our analysis suggests that long flanking introns are an intrinsic determinant of RNA circularization in pigs. Mammalian circRNAs have been reported to have relatively long flanking introns.<sup>7,33</sup> We aligned the introns of each intron pair that flanked a circRNA using the Basic Local Alignment Search Tool (BLAST). We observed that 1,810 circRNAs share RCMs of at least 100 bp in pigs (Fig. 2D). The lengths of long introns are not randomly distributed among circularized exons in the genome.<sup>8</sup> Short intronic repeat sequences and complementary sequences facilitate RNA circularization.<sup>3,38</sup> In our study, few circRNAs flanking intronic repeat sequences were detected, but the RCMs detected in our experiments are longer than previously reported RCMs; these characteristics may be typical of *S. scrofa* circRNAs.

### 3.4. circRNA isoforms and diversity of circularization pattern

Most genes generated one or two circRNAs, but some genes yielded multiple distinct circularized products (Fig. 3A). We identified 4,928 circRNAs generated from 2,538 annotated host genes. Among the identified circRNAs, 85.7% are produced by 'hot-spot' host genes that generate more than two circRNAs. This finding has been reported in other studies of circRNAs.<sup>3,5,8</sup> A striking example is the chromodomain

helicase DNA binding protein 2 gene (*CHD2*), which is involved in epigenetic regulation of chromatin structure and may generate as many as 40 distinct circRNAs (at least two unique back-spliced reads). CircRNA isoforms provide insight into the mechanism of circRNA biogenesis and the manner in which circRNAs are regulated. It is notable that, because de novo circRNA detection was performed without prior knowledge of annotated exons, 1,006 of the identified circRNAs fall outside the genomic regions of annotated genes.

There are structural complexities among well-expressed circRNAs. circRNAs produced from back-splicing have splicing signals at their junctions.<sup>4</sup> Introns spliced by the major spliceosome usually contain the GT dinucleotide at their 5' end (the splice donor) and the AG dinucleotide at their 3' end (the splice acceptor).<sup>40</sup> Most circRNAs contain one or a few exons; however, many circRNAs are supported by abundant back-spliced reads that traverse multiple exons. More than one GT donor site often exists for a given AG acceptor splicing site. We found that this situation is common when GT donors are more than one exon away from AG acceptor sites; such genes generate multiple circular RNAs. For example, *DIS3L2*, an important factor in mRNA degradation,<sup>41,42</sup> regulates Let-7g expression and apoptosis by targeting *TGFBR1* and down-regulating the activity of *TGF-β* pathway.<sup>43</sup> In our study, the *DIS3L2* gene was found to yield three circRNA isoforms, ssc-ciR-05526, ssc-ciR-05527, and ssc-ciR-05528, of 349 bp, 523 bp, and 603 bp in length, respectively (Fig. 3B). The circular fractions of ssc-ciR-05526, ssc-ciR-05527, and ssc-ciR-05528 (ratio of the circular isoform relative to all transcripts from the same locus) are 3.8, 23.2, and 17.3%, respectively. Many circRNAs have different acceptors, but share the same donor. For example, host gene *RBM25* produces two circRNA isoforms as shown in Fig. 3C. This analysis suggests the existence of alternative and interleaved splicing events, where the same splice sites can participate in multiple forward and backward splicing reactions, either to adjacent exons or to distant skipped exons.

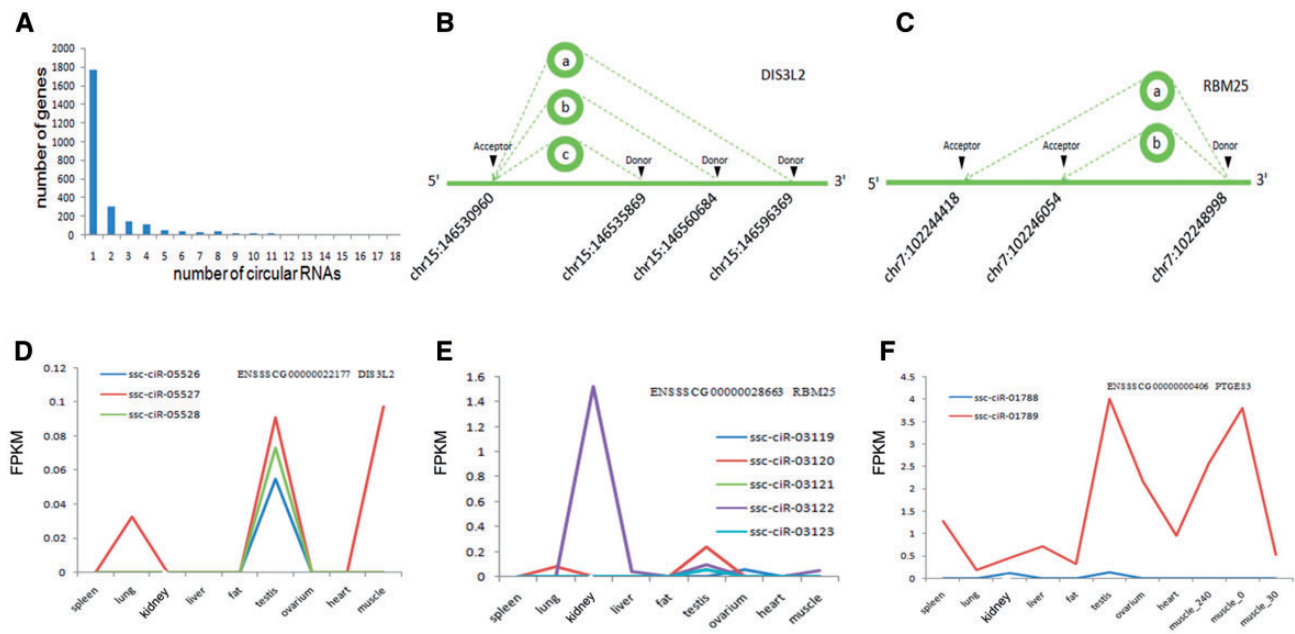


**Figure 3.** Generation model and examples of circRNAs isoform in pig. **(A)** Distribution of circular RNAs among genes; **(B)** The genome location of three deduced donors for one acceptor to generate circRNA in *DIS3L2*. **(C)** The genome location of two deduced acceptors for one donor to generate circRNA in *RBM25*. **(D)** Expression profile of three circRNA isoforms for *DIS3L2* in nine tissues. **(E)** *ssc-cir-03122* is abundantly expressed in kidney. **(F)** Tissue and age-dependent differential expression for two circRNA isoforms in *PTGES3*.

We further assessed the abundance of circRNA isoforms, revealing dissimilar expression profiles among different circRNAs originating from the same host gene. Expression profiles of this type have also been observed by other groups.<sup>8,44</sup> For example, among the three circRNA isoforms of *DIS3L2*, *ssc-cir-05527* is highly expressed in the lung, testis, and skeletal muscle at D240, whereas *ssc-cir-05526* and *ssc-cir-05528* were only detected in the testis (Fig. 3D). *ssc-cir-03122*, the predominant circRNA from the *RBM25* gene, is abundantly expressed in the kidney, while its other four circRNA isoforms are weakly expressed or not detected in most tissues (Fig. 3E). Among circRNA isoforms generated from *PTGES3*, *ssc-cir-01789* is widely expressed in all tissues and abundantly expressed in the testis and skeletal muscle. Expression of *ssc-cir-01789* in skeletal muscle was age-dependent. However, *ssc-cir-01788* from *PTGES3* is weakly expressed only in the kidney and testis (Fig. 3F). Another study revealed that some host genes produce multiple circRNAs with dissimilar expression profiles.<sup>45</sup> Collectively, these results suggest that back-splicing by alternative spliceosomes generates circRNA isoforms and contributes to the diversity and functional complexity of circRNAs.

### 3.5. *S. scrofa* circRNAs potentially act as miRNA sponges

A previous study indicated that circRNAs function as miRNA sponges to indirectly regulate mRNA expression.<sup>2,10</sup> To assess whether pig circRNAs regulate gene transcription by binding to miRNAs, we predicted miRNA binding sites of circRNAs using computational methods. We found 4,436 (74.8%), 4,432 (74.7%), and 2,279 (38.4%) putative miRNA-binding sites on 5,394 circRNAs using the microrna, RNAhybrid, and microtar programs, respectively (Supplementary Table S4, Fig. 4A). Moreover, we observed a significant positive relationship between the number of miRNA binding sites and circRNA length (Supplementary Fig. S2). To reduce the number of predicted false-positive miRNA targets, only miRNAs

considered as targets of circRNAs identified using all three programs were further assessed in our study. We identified 1,842 circRNAs with miRNA binding sites that were predicted by all three prediction methods (Fig. 4B); while most circRNAs were predicted to have no potential binding sites (Supplementary Table S4). The miRNA-binding sites were not equally distributed in the circRNAs, only 441 circRNAs out of 1842 (22.20%) had more than 20 potential binding sites (Fig. 4C).

Subsequently, we analysed interactions between differentially expressed circRNAs and predicted target miRNAs. The resulting circRNA–miRNA association network provided nodes and connections between circRNAs and their target miRNAs. According to our data, no miRNA was regulated by only one circRNA. For example, miRNA-378 is involved in a regulatory pathway for circRNA *ciR-90*. In total, 141 miRNAs and 81 circRNA host genes were involved in this network (Fig. 4D). These results suggest that circRNAs could regulate gene expression by functioning as miRNA sponges. We found that each circRNA can contain more than one miRNA binding site and can bind to more than one miRNA. Although these *in silico* results should be investigated *in vivo*, these results illuminate the manner in which circRNAs regulate mRNA translation.

### 3.6. Dominant circRNAs are expressed in a tissue-specific manner and highly enriched in the testis

To act as miRNA sponges or perform other non-catalytic cellular functions, circRNAs must be expressed at a consequential level within a cell or region of tissue.<sup>4</sup> Here, in order to gain insight into the circRNA landscape across different organs and infer the abundance of each circRNA, we multiplied the circular fraction of each circRNA by the density of RNA-seq reads arising from the cognate gene locus (measured in fragment per kilobase of transcript per million fragments sequenced, or FPKM) (Supplementary Table S5). Most circRNAs are expressed with relatively low abundance.<sup>4,46</sup>

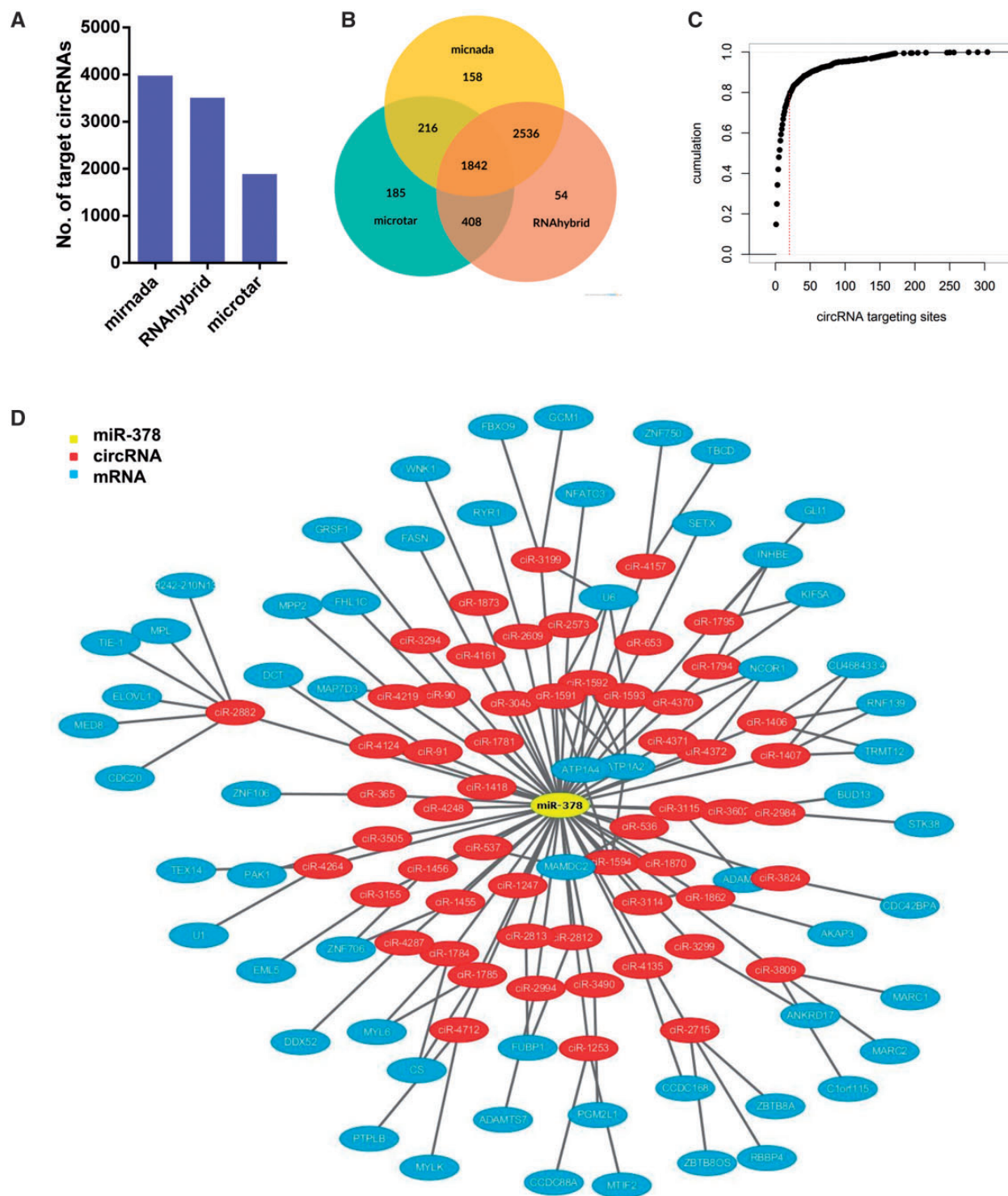


**Figure 4.** Analysis for circRNAs with the properties of miRNA sponges. **(A)** Prediction results of miRNA binding sites for circRNA by mirnada, RNAhybrid, and microtar program, respectively. **(B)** Overlapping of miRNA binding sites for circRNAs among three methods. **(C)** Number of miRNA binding sites for circRNAs. **(D)** A view of interaction between miRNA and circRNAs.

In this study, the average abundance of each *S. scrofa* circRNA was 0.45 FPKM. When considering the 395 circRNAs with inferred FPKM  $\geq 1.0$ , only 43 had FPKM  $\geq 10.0$ , while 4 had FPKM  $\geq 100$ . To test whether circRNAs are expressed in a tissue-specific manner in pigs, a clustered heatmap was generated for nine organs (Fig. 5A

and Supplementary Fig. S3). These results suggest that pig circRNAs have highly tissue-specific expression patterns (Fig. 5A). The largest cluster of circRNAs was in the testis and appeared to be testis-specific (Fig. 5A). Interestingly, circRNA ssc-ciR-03062, which is generated from *MYH7* and *MYH6*, which are associated with familial

hypertrophic cardiomyopathy,<sup>47,48</sup> was the most abundantly expressed circRNA in the heart and was highly expressed in skeletal muscle.

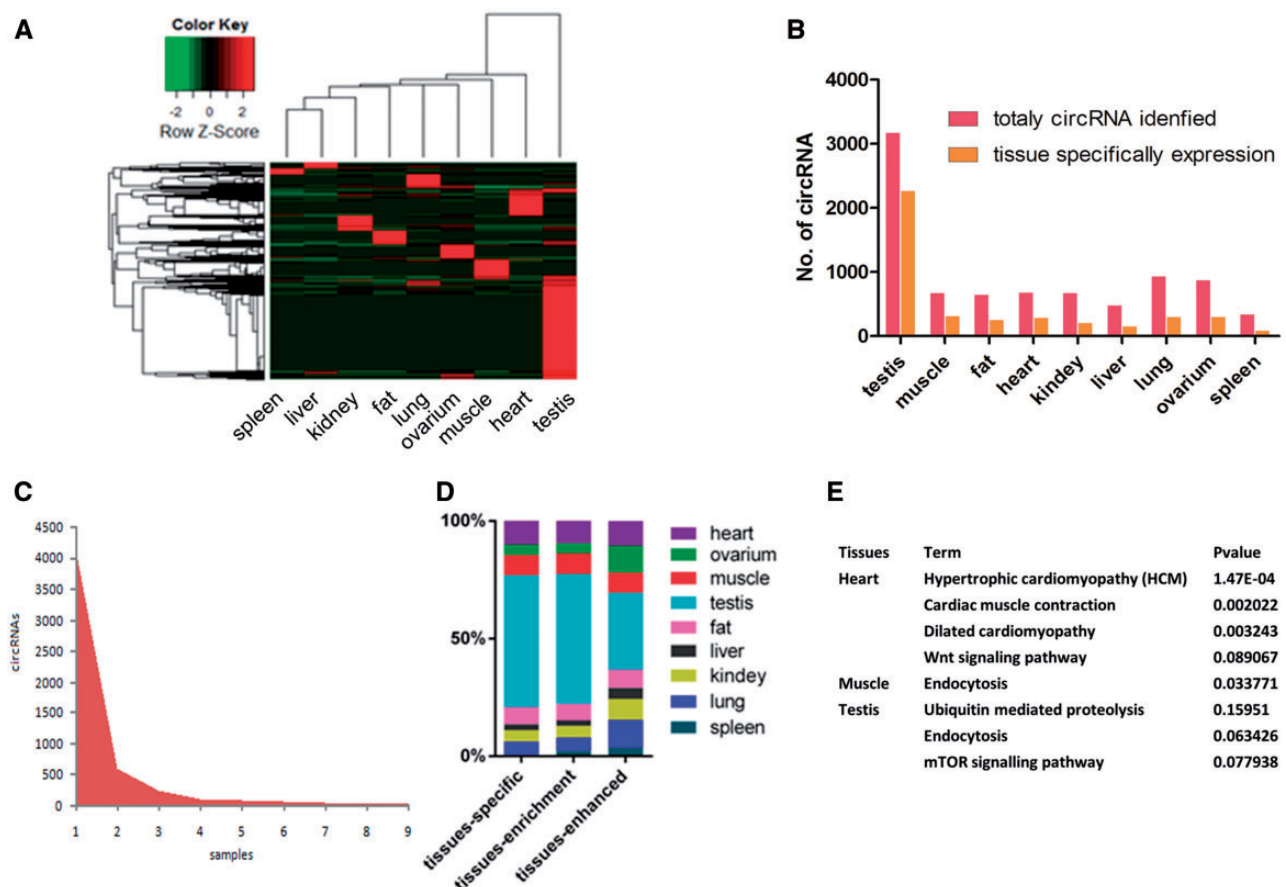
We found that 339–3,169 circRNAs were detected across most tissues types, and the testis had more than nine times as many circRNAs as the spleen (Fig. 5B). Some circRNAs are ubiquitously expressed, but most are found in only a few tissue types (Fig. 5C). We found that only 37 circRNAs are expressed in all nine organs analysed in this study. This variation was not explained by differences in sequencing depth. It is notable that 53.86% of the identified circRNAs ( $3,196/5,934 = 53.86\%$ ) were detected in the testis; however, 70.86% ( $2,265/3,196 = 70.86\%$ ) of the identified circRNAs were only observed in one other tissue type (Fig. 5B). Tissue-specific circRNAs are a group of circRNAs whose function and expression are confined to one or several tissues.<sup>49,50</sup> As shown in Supplementary Table S6, the testis shows the largest number of tissue-specific circRNAs (1,155), followed by the heart (205 circRNAs), muscle (174 circRNAs), and fat (147 circRNAs). The lowest number of tissue-specific circRNAs was found in the liver (53 circRNAs) (Table 1). It is notable that we did not detect any spleen-specific circRNAs. We assessed enrichment of gene ontology (GO) and Kyoto Encyclopaedia of Genes and Genomes (KEGG) terms among the tissue-specific circRNAs. In the heart, GO terms related to muscle development, construction, cell differentiation, and actin filament-based processes are highly enriched (Supplementary

Table S7). Pathway analysis indicates that the set of circRNAs specific to the heart is significantly enriched in genes related to hypertrophic cardiomyopathy (HCM), cardiac muscle contraction, dilated cardiomyopathy, and the *Wnt* signalling pathway (Fig. 5E).

Furthermore, we also analysed tissue-enriched (expression level at least 5-fold higher in a particular tissue as compared to all other tissues<sup>51</sup>) and tissue-enhanced (at least 5-fold higher expression level in a particular tissue as compared to the average level in all tissues<sup>51</sup>) circRNA. We identified 2,167 tissue-enriched circRNAs (Supplementary Table S8) and 3,301 tissue-enhanced circRNAs (Supplementary Table S9) across all nine assessed tissue types. The numbers of tissue-enriched and tissue-enhanced genes are highly variable among the analysed tissue types (Table 1, Fig. 5D). The testis shows the largest number of tissue-enriched circRNAs (1,192), followed by the heart (223) and skeletal muscle (186). These results indicate that circRNAs are expressed with highly tissue-specific patterns in pigs. A previous study also reported that dominant circular RNAs were expressed in a tissue-specific manner during human fetal development.<sup>9</sup>

### 3.7. Differentially expressed circRNAs in postnatal skeletal muscle

Skeletal muscles allow movement of the body via energy expenditure. Postnatal growth of skeletal muscle is mainly realized through increases in the length and girth of muscle fibres, but not by increases



**Figure 5.** The tissue-specific expression of *S. scrofa* circRNAs in pigs. (A) Hierarchical clustering of the circular fraction of 5,399 circRNAs expressed in nine tissues with  $\geq 2$  reads. (B) Numbers of circRNAs identified each tissues. (C) Number of *S. scrofa* circRNAs in tissues analysed. (D) Percentage of tissues specific, -enrichment, and -enhanced circRNAs in each tissues. (E) KEGG term enrichments of circRNAs reveal many genes sets that were specific in tissues.

**Table 1.** Classification of circRNA expression in different tissues

Tissues	Tissues-specific circRNAs	Tissues-enrichment circRNAs	Tissues-enhanced circRNAs
Spleen	0	49	182
Lung	130	125	568
Kidney	99	106	433
Liver	53	53	232
Fat	147	149	371
Testis	1,155	1,192	1,596
Muscle	174	186	412
Ovarium	94	95	555
Heart	205	223	512

in muscle fibre number.<sup>52</sup> To understand the regulation of circRNAs in skeletal muscle, we performed expression profiling of circRNAs in skeletal muscle at postnatal days 0, 30, and 240 (designated D0, D30, and D240, respectively). This profiling allowed evaluation of dynamic changes in circRNA expression from birth until adulthood and identification of circRNAs associated with muscle growth. We detected 1,489 circRNAs expressed with more than two reads in at least one sample (Supplementary Table S10). Of these 1,489 skeletal muscle circRNAs, 597 circRNAs were detected at D0, whereas 670 were detected at D30 and 673 were detected at D240; 57.2–63.9% of skeletal muscle circRNAs were detected at only one stage (Fig. 6A). The identified skeletal muscle circRNAs were studied further to assess changes in their expression levels during skeletal muscle growth. To obtain an overview of spatial circRNA expression changes in developmental skeletal muscle, we clustered pig circRNA expression data from D0, D30, and D240, revealing differential circRNA expression between growth stages. Interestingly, cluster analysis showed that skeletal muscle at D30 had a circRNA expression profile more similar to that of skeletal muscle at D240 than to that of skeletal muscle at D0 (Fig. 6B).

Next, we focused on abundant circRNAs in skeletal muscle. Notably, we found that several of the most abundant circRNAs in skeletal muscle originate from protein coding genes with pivotal roles in skeletal muscle growth and hypertrophy (e.g. *MYH1*, *MYH2*, *MYH3*, *MYH6*, *MYH7*, *MYL12B*, *IGFBP5*) or non-coding RNAs with roles in slow-twitch fibre formation (miRNA-208b encoded by introns of myosin genes) (Fig. 6C).<sup>53,54</sup> *MYH1*, *MYH6*, and *MYH7* belong to the *MYH* myosin superfamily. Myosin, the primary component of thick filaments, is widely expressed in mammalian skeletal muscle and involved in muscle contraction, phagocytosis, cell motility, and vesicle transport.<sup>55,56</sup> Recent studies reported that myosins are associated with skeletal muscle development and influence the quality of pork.<sup>57–59</sup> We analysed the expression patterns of all circRNAs detected in skeletal muscle, revealing 16 expression patterns and significant enrichment in cluster 5 (Supplementary Fig. S3). GO analysis of circRNAs expressed in skeletal muscle did not reveal significant enrichment in GO terms.

To study functional transitions in skeletal muscle development, we assessed two types of differentially expressed circRNAs (DEC) between time points. We focused on circRNAs with fold-change >2, *P*-value < 0.05, and FDR < 0.1. The expression levels of most circRNAs are not significantly altered during postnatal skeletal muscle growth. Type 1 DECs were defined as those that were differentially expressed between two closed time points. We detected 101 and 83 differentially expressed circRNAs in the D0 versus D30 and D30 versus D240 analyses, respectively. Among these DECs, 75 circRNAs

were up-regulated at D30 in comparison with D0, whereas 26 circRNAs were up-regulated at D0 in comparison with D30 (Supplementary Table S11, Fig. 6D). In the D30 versus D240 group, 58 circRNAs were up-regulated at D240 in comparison with D30, whereas 25 circRNAs were up-regulated at D30 in comparison with D240 (Supplementary Table S12, Fig. 6E). Under the assumption that the functions of circRNAs are related to the functions of their host genes, we performed GO and KEGG pathway analysis to predict the functions of DECs during postnatal growth of skeletal muscle. The GO analysis indicated that the host genes of the D0 versus D30 DECs are significantly associated with muscle development (Supplementary Fig. S4A). However, for the D30 versus D240 DECs, host genes are associated with homeostatic processes such as ion homeostasis and cation homeostasis (Supplementary Fig. 4B). Pathway analysis indicated that the host genes of the D0 versus D30 DECs are involved in tight junction signalling (Table 2). In the D30 versus D240 group, circRNA host genes are significantly associated with the calcium signalling pathway and aldosterone-regulated sodium reabsorption signalling pathway. The overall induction of circRNAs during skeletal muscle development indicates that circularization is likely important for muscle function, because many circRNAs are up- or down-regulated at different time points of skeletal muscle growth.

Type 2 DECs were defined as circRNAs that were differentially expressed only in the D0 versus D30 or D30 versus D240 analyses, representing circRNAs that were up- or down-regulated only between two consecutive time points during muscle growth. We found 29 circRNAs that were differentially expressed in the D0 versus D30 comparison, but not in the D30 versus D240 comparison (Supplementary Table 13). Notably, several circRNAs generated from *MYH1*, *MYH2*, *MYH6*, *MYH7*, and *TNNC2*, as well as miRNA-208b, were significantly differentially expressed only in the D0 versus D30 comparison. These host genes mainly encoded proteins associated with muscle development and fibre twitching. We found 24 circRNAs that were differentially expressed in the comparison of D30 and D240, but not in the comparison of D0 and D30 (Supplementary Table S14). Interestingly, these circRNAs were mainly generated from *NDFIP2*, *RBM6*, *RYR1*, *SEC24A*, *RYR1*, *RBM24*, *SAR1B*, *PLEKHF1*, *ATP1A2*, *ATP1A4*, *DCUN1D1*, *ATP1A2*, *PRSS22*, and *PHKB*, which encode proteins associated with glycosaminoglycan metabolism and calcium channels. These circRNAs could signify the onset/termination of growth and/or physiological processes at a particular developmental stage.

### 3.8. *S. scrofa* circRNA database

In order to facilitate dissemination of information regarding circRNA annotation, circRNA expression, potential circRNA functions, and circRNA–miRNA–gene interactions, we created a database of *S. scrofa* circRNAs that was designated pigcirNet (<http://lnc.rnanet.org/circ>). The web interface of pigcirNet is summarized in Fig. 7. PigcirNet shows circRNA location, circular nucleotide length, strand signal, gene Entrez ID, Ensembl id, gene symbol, classification, and expression level across all organs and stages selected in this study. Information regarding prediction of circRNA targeting by miRNAs and circRNA–miRNA interactions are also available in pigcirNet. In order to investigate potential functions of circRNAs, we retrieve GO information with host-related genes. We also search the PubMed database to retrieve reports related to queried circRNAs. A Google<sup>®</sup> chart is used to display a diagram of circRNA abundance, whereas sigma.js is used to show a circRNA, mRNA, and miRNA interaction network. circRNAs can be browsed by their



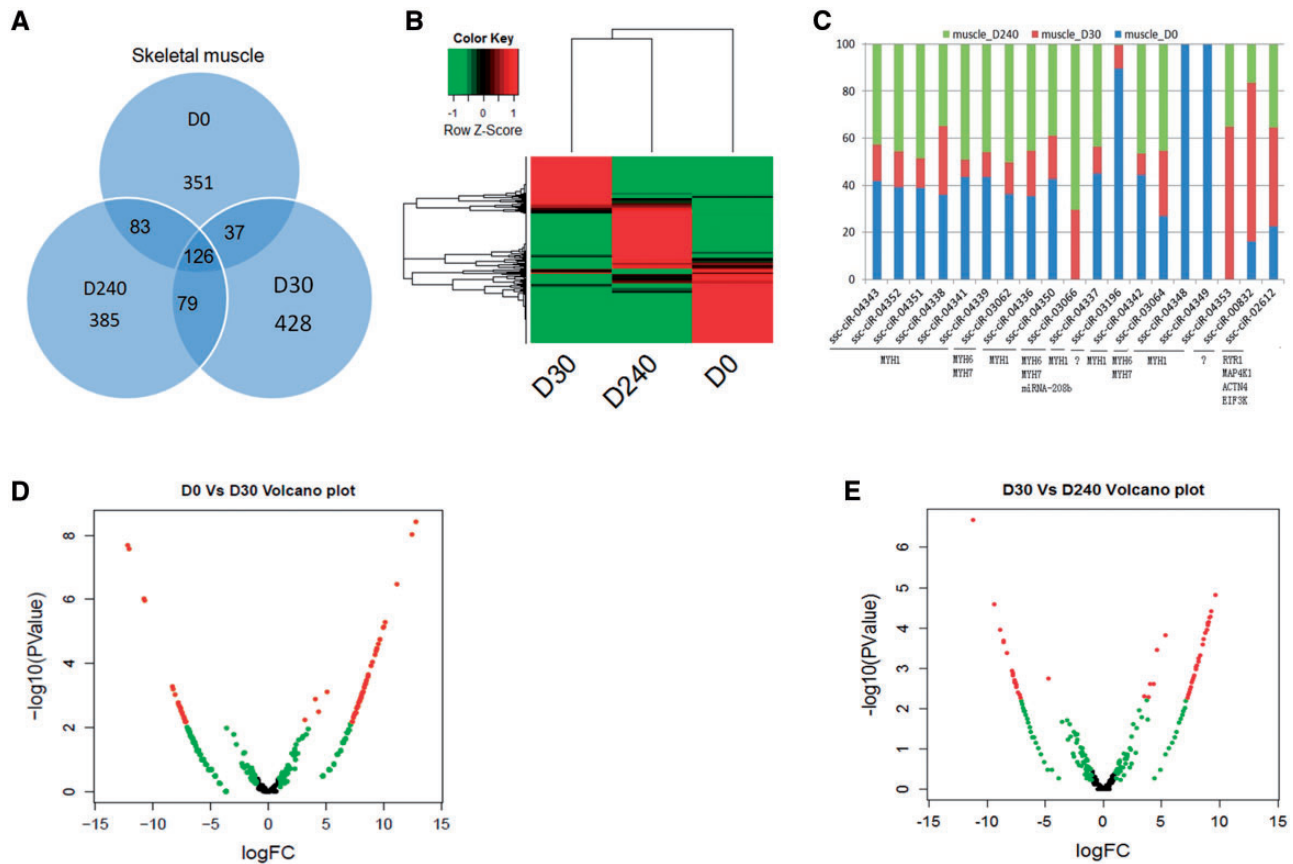


**Figure 6.** Temporal expression of circRNAs in skeletal muscle. **(A)** Venn chart of circRNAs detected in skeletal muscle. **(B)** Heatmap of circRNA expression abundance at 0 day, 30 days, and 240 days. **(C)** Top circRNAs expressed in skeletal muscle. **(D–E)** Differentially expressed circRNA between different growth stages in postnatal skeletal muscle.

**Table 2.** Pathway analysis of parent genes of circRNAs

Group	Term	<i>P</i> value	Benjamini <i>q</i> value
D0 versus D30	Tight junction	7.67E–05	0.0029
D30 versus D240	Calcium signalling pathway	0.0365	0.67
D30 versus D240	Aldosterone-regulated sodium reabsorption	0.0703	0.66

Note: Significantly over-represented KEGG (Kyoto Encyclopaedia of Genes and Genomes) pathways detected with DAVID for parent genes of circRNAs that are differentially expressed with at least a twofold changes in group D0 versus D30 and D30 versus D240, respectively.

chromosomal location, classification, or tissue-specific expression pattern. We also provide a search box, in which users can find related circRNAs by searching circRNA id, gene symbol, gene Entrez ID, or gene Ensembl ID. To the best of our knowledge, our database is the first public circRNA resource for a non-rodent mammal.

#### 4. Discussion

Genome-wide analyses of RNA-seq data have revealed that circRNAs are abundant in animal transcriptomes and identified thousands of circRNAs in humans,<sup>2,60</sup> mice,<sup>4</sup> nematodes,<sup>2</sup> and drosophila.<sup>7,37</sup> Guo

et al. detected 7,112 human circRNAs using 39 biological samples of whole-cell non-poly(A)-selected RNA-seq data from the ENCODE project.<sup>4</sup> Gao et al. applied the CIRI algorithm to identify nearly 98,526 circRNAs based on ENCODE RNA-seq data from 15 cell lines.<sup>60</sup> Based on 464 RNA-seq samples across 26 human tissues and 104 disease conditions,<sup>61</sup> Liu and colleagues identified 212,950 human circRNAs (53,687 novel circRNAs). These findings suggest that a large number of circRNAs remain unknown and indicate that additional circRNAs can be identified by improving RNA analysis methods and accumulating deeper sequencing data. Because circRNAs are expressed in a highly spatio-temporal specific manner, it is essential that studies of circRNAs in mammals assess various tissues, conditions, and developmental stages. The pig is an important farm animal that provides protein for humans and an important non-rodent animal model that is widely used in biomedical research. Morten et al., the first group to study *S. scrofa* circRNAs, identified 4,634 unique circRNAs from 2,195 host genes in five brain tissue types at six time-points during fetal porcine development, and the results suggested that some circRNAs were conserved between humans and mice.<sup>8</sup> To perform genome-wide identification of *S. scrofa* circRNAs and explore their spatio-temporal expression patterns, we carried out total RNA sequencing across nine organs (heart, liver, spleen, lung, kidney, ovary, testis, skeletal muscle, and fat) and skeletal muscle at three developmental stages (0, 30, and 240 days after birth). We identified 5,934 *S. scrofa* circRNAs, which represent a significant addition to the growing catalogue of annotated mammalian circRNAs. The

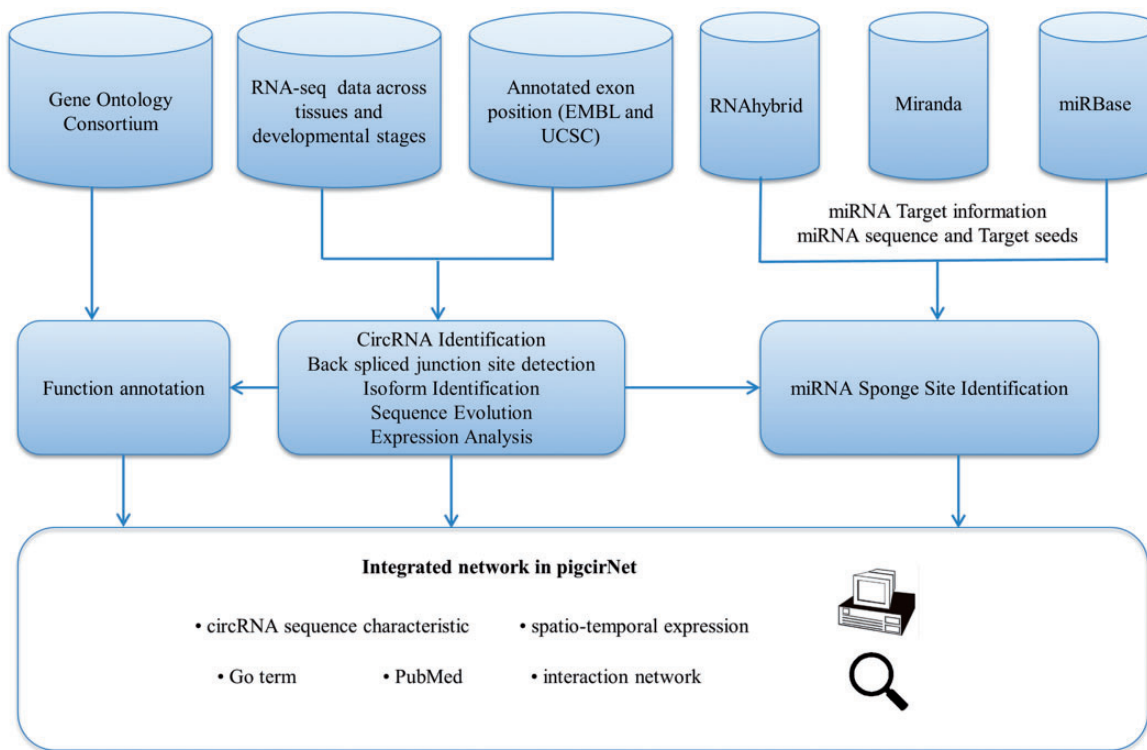


**Figure 7.** Framework of the database construction in pigcirNet. The graph illustrates how the network in pigcirNet was constructed.

circRNAs *CDR1as* and *Sry* were well-known studied. However, we did not detect circRNAs formed by a *CDR1as* orthologue or *Sry* in our data. *Sry* is induced during embryonic development.<sup>62</sup> Because circRNAs are expressed in a tissue- and cell-specific manner, *S. scrofa* circRNAs orthologous to *CDR1as* and *Sry* were probably not expressed in the tissues selected in our study. To validate this conjecture, we further analysed expression of *CDR1* and *Sry*. As expected, we did not detect expression of *CDR1* or *Sry* in any tissue. Neither *CDR1* nor *Sry* were mentioned in Morten's study of the pig brain,<sup>8</sup> indicating that these circRNAs were not expressed in these samples. We analysed a limited set of tissues and developmental stages in this study. Thus, the true number of *S. scrofa* circRNAs is almost certainly much larger than that reported in this study. In comparison with humans, knowledge of *S. scrofa* circRNAs remains limited. Therefore, deeper RNA-sequencing to identify circRNAs across additional organs and developmental stages in pigs is essential.

Although the molecular functions of circRNAs are mostly unclear, some circRNAs affect gene expression by acting as microRNA sponges. The most emblematical examples of circRNAs that act as microRNA sponges are *CDR1as/ciRS-7* and *Sry*, which function in human and mouse brain development.<sup>2,10</sup> Guo et al. predicted that circRNAs from the human C2H2 zinc finger gene family function as miRNA sponges.<sup>4</sup> Another study showed that *Drosophila* circular RNAs harbour >1000 well-conserved canonical miRNA seed matches.<sup>7</sup> To assess whether *S. scrofa* circRNAs affect post-transcriptional gene regulation by binding to miRNAs, we predicted circRNA-originating targets by three computational methods. We found that 1,842 of 5,934 (31.04%) circRNAs had putative miRNA-binding sites. In a study of rice, 17.33% (235/1356) of circRNAs were found to have putative miRNA-binding sites.<sup>63</sup> The identified circRNAs had, on average, 19 miRNA-binding sites. There was a significant positive relationship between the number

of miRNA-binding sites and circRNA sequence length (Supplementary Fig. S2). Based on our analysis of circRNAs, we constructed an interaction network of miRNAs and circular RNAs. Certainly, the potential genome-wide interplay between miRNAs and circular RNAs warrants further experimental and computational investigation in the future. Although the aforementioned studies indicated that some circRNAs function as miRNA sponges, 4,092 of 5,934 (68.96%) *S. scrofa* circRNAs identified in this study have no putative miRNA binding site. Several studies have suggested that most circRNAs do not act as miRNA sponges.<sup>4,63</sup> These findings indicate that circRNAs have functions other than binding to miRNAs, including regulation of host gene transcription, protein binding, and translation.<sup>11,64</sup>

Spatio-temporal gene expression patterns reveal the functions of genes within specific tissues/cells at specific times during development. Several studies have revealed that circRNAs tend to show tissue-/stage-specific expression<sup>7-9</sup> and enrichment in the brain.<sup>35</sup> We also identified tissue-specific, tissue-enriched, and tissue-enhanced circRNAs, providing important information regarding their functions. Of the identified heart-specific circRNAs, for example, *ssc-ciR-03925*, *ssc-ciR-03394*, *ssc-ciR-03072*, *ssc-ciR-05708*, *ssc-ciR-02839*, *ssc-ciR-02761*, *ssc-ciR-04971*, *ssc-ciR-04972*, and *ssc-ciR-03852* were specifically expressed in the heart. *ssc-ciR-04971* is generated from host gene *RYR2*, mutations in which are associated with stress-induced polymorphic ventricular tachycardia and arrhythmogenic right ventricular dysplasia.<sup>65</sup> *Ssc-ciR-03072* is produced from host gene *MYH7*, changes in the relative abundance of which are correlated with the contractile velocity of cardiac muscle; mutations in *MYH7* are associated with familial hypertrophic cardiomyopathy, myosin storage myopathy, dilated cardiomyopathy, and Laing early onset distal myopathy.<sup>66,67</sup> These findings suggest that heart-specific circRNAs might be involved in heart development and cardiac disease.

Skeletal muscle mass increases during postnatal animal development via hypertrophy.<sup>68</sup> The role of circRNAs in skeletal muscle development is unknown. Therefore, we analysed dynamic changes in circRNA abundance during postnatal growth of skeletal muscle. We identified 149 circRNAs that were differentially expressed between the selected time points and thus might be associated with postnatal growth of skeletal muscle. No studies have assessed the role of circRNAs in myogenesis. The D0 versus D30 DECs and D30 versus D240 DECs differed significantly with respect to enriched GO terms and signalling pathways. The D0 vs. D30 DECs were markedly enriched in GO terms associated with muscle contraction, muscle organ development, and chromatin modification, while the D30 versus D240 DECs were enriched in GO terms associated with cellular cation homeostasis, ATP hydrolysis-coupled proton transport, energy-coupled proton transport against the electrochemical gradient, and response to hypoxia. KEGG analysis suggested that DECs were mainly enriched in the tight junction pathway for the D0 versus D30 group, while DECs in the D30 versus D240 group were significantly associated with calcium signalling and aldosterone-regulated sodium reabsorption signalling. Tight junction proteins participate in the regulation of cell proliferation, gene expression, and cell differentiation.<sup>69,70</sup> A previous study showed that proliferation and fusion of satellite cells, leading to an increase in the number of myonuclei, may also regulate muscle growth during the early, but not late, stages of postnatal development.<sup>68</sup> Our study indicated that circRNAs (such as ssc-ciR-02753, ssc-ciR-04353, ssc-ciR-04335, ssc-ciR-04349, ssc-ciR-04348, ssc-ciR-04359, ssc-ciR-03066, ssc-ciR-03069, and ssc-ciR-03065) may regulate muscle growth by affecting cell proliferation and fusion during early postnatal muscle development. Clustering analysis suggested that the circRNA expression profile of skeletal muscle at D30 was more similar to that of skeletal muscle at D240 than to that of skeletal muscle at D0. We speculate that circRNAs such as ssc-ciR-01595, ssc-ciR-01592, ssc-ciR-03395, ssc-ciR-02589, ssc-ciR-02611, and ssc-ciR-02610 contribute to muscle plasticity and contraction. Some circRNAs are evolutionarily conserved in terms of sequence and expression, suggesting that they possess similar cellular functions in diverse species.<sup>34,35,71</sup> Our genome-wide analysis of the spatio-temporal expression patterns of *S. scrofa* circRNAs provides a foundation for studies aimed at understanding the molecular functions of mammalian circRNAs.

Thousands of circRNAs have been discovered in plants, animals, and humans. Given the emerging understanding of the biological importance of circRNAs and research efforts to understand them, researchers have constructed several circRNA databases, including Circ2Traits,<sup>72</sup> CircNet,<sup>61</sup> deepBase v2.0,<sup>73</sup> CircInteractome,<sup>74</sup> and SomamiR2.0.<sup>75</sup> At present, these databases include human, mouse, and *C. elegans* circRNAs, but not *S. scrofa* circRNAs, because identification of circRNAs in pigs has lagged far behind identification of circRNAs in humans, mice, and *C. elegans*. Exploring the pig genome can illuminate facets of human culture, organic evolution, biomedical research, and animal breeding. Therefore, we constructed the database of *S. scrofa* circRNAs based on our data. To the best of our knowledge, this database is the first public resource containing information about the circRNAs of a non-rodent mammal.

## Availability

RNA-seq data were deposited in the Gene Expression Omnibus with accession codes was GSE73763. The identified circRNA was stored in <http://lnc.rnanet.org/circ>.

## Acknowledgements

This work was supported by National Key Basic Research Program of China (2014CB138504, 2015CB943101), National Natural Science Foundation of China (31171192, 31330074), the Agricultural Science and Technology Innovation Program (ASTIP-IAS16). This work was also supported by Key Laboratory of Shenzhen (ZDSYS20141118170111640).

## Supplementary data

Supplementary data are available at [www.dnaresearch.oxfordjournals.org](http://www.dnaresearch.oxfordjournals.org).

## Conflict of interest

None declared.

## References

- Hsu, M.-T. and Coca-Prados, M. 1979, Electron microscopic evidence for the circular form of RNA in the cytoplasm of eukaryotic cells, *Nature*, **280**, 339–40.
- Memczak, S., Jens, M., Elefsinioti, A., et al. 2013, Circular RNAs are a large class of animal RNAs with regulatory potency, *Nature*, **495**, 333–8.
- Zhang, X.-O., Wang, H.-B., Zhang, Y., Lu, X., Chen, L.-L. and Yang, L. 2014, Complementary sequence-mediated exon circularization, *Cell*, **159**, 134–47.
- Guo, J. U., Agarwal, V., Guo, H. and Bartel, D. P. 2014, Expanded identification and characterization of mammalian circular RNAs, *Genome Biol.*, **15**, 014–0409.
- Fan, X., Zhang, X., Wu, X., et al. 2015, Single-cell RNA-seq transcriptome analysis of linear and circular RNAs in mouse preimplantation embryos, *Genome Biol.*, **16**, 148.
- Ye, C.-Y., Chen, L., Liu, C., Zhu, Q.-H. and Fan, L. 2015, Widespread noncoding circular RNAs in plants, *New Phytol.*, **208**, 88–95.
- Westholm, J.O., Miura, P., Olson, S., et al. 2014, Genome-wide analysis of Drosophila circular RNAs reveals their structural and sequence properties and age-dependent neural accumulation, *Cell Rep.*, **9**, 15.
- Veno, M. T., Hansen, T. B., Veno, S. T., et al. 2015, Spatio-temporal regulation of circular RNA expression during porcine embryonic brain development, *Genome Biol.*, **16**, 015–0801.
- Szabo, L., Morey, R., Palpant, N. J., et al. 2015, Statistically based splicing detection reveals neural enrichment and tissue-specific induction of circular RNA during human fetal development, *Genome Biol.*, **16**, 015–0690.
- Hansen, T. B., Jensen, T. I., Clausen, B. H., et al. 2013, Natural RNA circles function as efficient microRNA sponges, *Nature*, **495**, 384–8.
- Li, Z., Huang, C., Bao, C., et al. 2015, Exon-intron circular RNAs regulate transcription in the nucleus, *Nat. Struct. Mol. Biol.*, **22**, 256–64.
- Kumar, S. and Hedges, S. B. 1998, A molecular timescale for vertebrate evolution, *Nature*, **392**, 917–20.
- Larson, G., Dobney, K., Albarella, U., et al. 2005, Worldwide phylogeography of wild boar reveals multiple centers of pig domestication, *Science*, **307**, 1618–21.
- Groenen, M. A., Archibald, A. L., Uenishi, H., et al. 2012, Analyses of pig genomes provide insight into porcine demography and evolution, *Nature*, **491**, 393–8.
- Wernersson, R., Schierup, M. H., Jørgensen, F. G., et al. 2005, Pigs in sequence space: a 0.66 X coverage pig genome survey based on shotgun sequencing, *BMC Genomics*, **6**, 1.
- Liu, Y., Ma, Y., Yang, J.-Y., et al. 2014, Comparative gene expression signature of pig, human and mouse induced pluripotent stem cell lines reveals insight into pig pluripotency gene networks, *Stem Cell Rev. Rep.*, **10**, 162–76.
- Wall, R. and Shani, M. 2008, Are animal models as good as we think?, *Theriogenology*, **69**, 2–9.

18. Walters, E. M., Wolf, E., Whyte, J. J., et al. 2012, Completion of the swine genome will simplify the production of swine as a large animal biomedical model, *BMC Med Genomics*, 5, 55.
19. Tuggle, C. K., Wang, Y. and Couture, O. 2007, Advances in swine transcriptomics, *Int. J. Biol. Sci.*, 3, 132–52.
20. Gorodkin, J., Cirera, S., Hedegaard, J., et al. 2007, Porcine transcriptome analysis based on 97 non-normalized cDNA libraries and assembly of 1,021,891 expressed sequence tags, *Genome Biol.*, 8, R45.
21. Tuggle, C. K., Green, J. A., Fitzsimmons, C., et al. 2003, EST-based gene discovery in pig: virtual expression patterns and comparative mapping to human, *Mamm. Genome*, 14, 565–79.
22. Zhao, Y., Li, J., Liu, H., et al. 2015, Dynamic transcriptome profiles of skeletal muscle tissue across 11 developmental stages for both Tongcheng and Yorkshire pigs, *BMC Genomics*, 16, 377.
23. Tang, Z., Li, Y., Wan, P., et al. 2007, LongSAGE analysis of skeletal muscle at three prenatal stages in Tongcheng and Landrace pigs, *Genome Biol.*, 8, R115.
24. Hou, X., Yang, Y., Zhu, S., et al. 2015, Comparison of skeletal muscle miRNA and mRNA profiles among three pig breeds, *Mol. Genet. Genomics*, 291, 559–15.
25. Tang, Z., Yang, Y., Wang, Z., Zhao, S., Mu, Y. and Li, K. 2015, Integrated analysis of miRNA and mRNA paired expression profiling of prenatal skeletal muscle development in three genotype pigs, *Sci. Rep.*, 5, 15544.
26. Langmead, B. and Salzberg, S. L. 2012, Fast gapped-read alignment with Bowtie 2, *Nat. Meth.*, 9, 357–9.
27. Li, H. 2011, A statistical framework for SNP calling, mutation discovery, association mapping and population genetical parameter estimation from sequencing data, *Bioinformatics*, 27, 2987–93.
28. Glazar, P., Papavasileiou, P. and Rajewsky, N. 2014, circBase: a database for circular RNAs, *RNA*, 20, 1666–70.
29. Kozomara, A. and Griffiths-Jones, S. 2014, miRBase: annotating high confidence microRNAs using deep sequencing data, *Nucleic Acids Res.*, 42, D68–73.
30. Thadani, R. and Tammi, M. T. 2006, MicroTar: predicting microRNA targets from RNA duplexes, *BMC Bioinformatics*, 7 Suppl 5, S20.
31. John, B., Enright, A. J., Aravin, A., Tuschl, T., Sander, C. and Marks, D. S. 2004, Human microRNA targets, *PLoS Biol.*, 2, e363.
32. Krüger, J. and Rehmsmeier, M. 2006, RNAhybrid: microRNA target prediction easy, fast and flexible, *Nucleic Acids Res.*, 34, W451–4.
33. Salzman, J., Chen, R. E., Olsen, M. N., Wang, P. L. and Brown, P. O. 2013, Cell-type specific features of circular RNA expression. *PLoS Genet.*, 9, e1003777.
34. Jeck, W. R., Sorrentino, J. A., Wang, K., et al. 2013, Circular RNAs are abundant, conserved, and associated with ALU repeats, *RNA*, 19, 426.
35. Rybak-Wolf, A., Stottmeister, C., Glazar, P., et al. 2015, Circular RNAs in the mammalian brain are highly abundant, conserved, and dynamically expressed, *Mol. Cell*, 58, 870–85.
36. Dang, Y., Yan, L., Hu, B., et al. 2016, Tracing the expression of circular RNAs in human pre-implantation embryos, *Genome Biol.*, 17, 1–15.
37. Ashwal-Fluss, R., Meyer, M., Pamudurti, Nagarjuna R., et al. 2014, circRNA biogenesis competes with pre-mRNA splicing, *Mol. Cell*, 56, 55–66.
38. Liang, D. and Wilusz, J. E. 2014, Short intronic repeat sequences facilitate circular RNA production, *Genes Dev.*, 28, 2233–47.
39. Starke, S., Jost, I., Rossbach, O., et al. Exon circularization requires canonical splice signals. *Cell Rep.*, 10, 103–111.
40. Sharp, P. A. and Burge, C. B. Classification of introns: U2-type or U12-type, *Cell*, 91, 875–9.
41. Faehnle, C. R., Walleshauser, J. and Joshua-Tor, L. 2014, Mechanism of Dis3L2 substrate recognition in the Lin28-let-7 pathway, *Nature*, 514, 252–6.
42. Malecki, M., Viegas, S. C., Carneiro, T., et al. 2013, The exoribonuclease Dis3L2 defines a novel eukaryotic RNA degradation pathway, *EMBO J*, 32, 1842–54.
43. Zhou, J., Liu, J., Pan, Z., et al. 2015, The let-7g microRNA promotes follicular granulosa cell apoptosis by targeting transforming growth factor- $\beta$  type 1 receptor, *Mol. Cell. Endocrinol.*, 409, 103–12.
44. Zheng, Q., Bao, C., Guo, W., et al. 2016, Circular RNA profiling reveals an abundant circHIPK3 that regulates cell growth by sponging multiple miRNAs, *Nat. Commun.*, 7, 11215.
45. Ameres, S. L. and Zamore, P. D. 2013, Diversifying microRNA sequence and function, *Nat. Rev. Mol. Cell Biol.*, 14, 475–88.
46. Chen, I., Chen, C.-Y. and Chuang, T.-J. 2015, Biogenesis, identification, and function of exonic circular RNAs, *Wiley Interdiscip. Rev. RNA*, 6, 563–79.
47. Bashyam, M. D., Purushotham, G., Chaudhary, A. K., et al. 2012, A low prevalence of MYH7/MYBPC3 mutations among Familial Hypertrophic Cardiomyopathy patients in India, *Mol. Cell. Biochem.*, 360, 373–82.
48. Hershberger, R. E., Norton, N., Morales, A., Li, D., Siegfried, J. D. and Gonzalez-Quintana, J. 2010, Coding sequence rare variants identified in MYBPC3, MYH6, TPM1, TNNC1, and TNNI3 from 312 patients with familial or idiopathic dilated cardiomyopathy, *Circ. Cardiovasc. Genet.*, 3, 155–61.
49. Lagos-Quintana, M., Rauhut, R., Yalcin, A., Meyer, J., Lendeckel, W. and Tuschl, T. 2002, Identification of tissue-specific microRNAs from mouse, *Curr Biol.*, 12, 735–9.
50. Guo, Z., Maki, M., Ding, R., Yang, Y., Zhang, B. and Xiong, L. 2014, Genome-wide survey of tissue-specific microRNA and transcription factor regulatory networks in 12 tissues, *Sci. Rep.*, 4, 5150.
51. Uhlen, M., Fagerberg, L., Hallstrom, B. M., et al. 2015, Proteomics. Tissue-based map of the human proteome, *Science*, 347, 1260419.
52. Dahmane Gošnjak, R., Erzen, I., Holcman, A. and Škorjanc, D. 2010, Effects of divergent selection for 8-week body weight on postnatal enzyme activity pattern of 3 fiber types in fast muscles of male broilers (*Gallus gallus domesticus*), *Poult. Sci.*, 89, 2651–9.
53. Drummond, M. J., McCarthy, J. J., Fry, C. S., Esser, K. A. and Rasmussen, B. B. 2008, Aging differentially affects human skeletal muscle microRNA expression at rest and after an anabolic stimulus of resistance exercise and essential amino acids, *Am. J. Physiol. –Endocrinol. Metab.*, 295, E1333–40.
54. Hitachi, K. and Tsuchida, K. 2014, Role of microRNAs in skeletal muscle hypertrophy, *Front. Physiol.*, 4, 408.
55. De La Cruz, E. M. and Ostap, E. M. 2004, Relating biochemistry and function in the myosin superfamily, *Curr. Opin. Cell Biol.*, 16, 61–7.
56. Akolkar, D. B., Kinoshita, S., Yasmin, L., et al. 2010, Fibre type-specific expression patterns of myosin heavy chain genes in adult torafugu Takifugu rubripes muscles, *J. Exp. Biol.*, 213, 137–45.
57. Lim, K.-S., Lee, S.-H., Lee, E.-A., Kim, J.-M. and Hong, K.-C. 2015, Effects of intergenic single nucleotide polymorphisms in the fast myosin heavy chain cluster on muscle fiber characteristics and meat quality in Berkshire pigs, *Meat Sci.*, 110, 224–9.
58. Zou, T., He, D., Yu, B., et al. 2015, Moderately increased maternal dietary energy intake delays foetal skeletal muscle differentiation and maturity in pigs, *Eur. J. Nutr.*, 55, 1777–87.
59. Xiong, X., Liu, X., Zhou, L., et al. 2015, Genome-wide association analysis reveals genetic loci and candidate genes for meat quality traits in Chinese Laiwu pigs, *Mamm. Genome*, 26, 181–90.
60. Gao, Y., Wang, J. and Zhao, F. 2015, CIRI: an efficient and unbiased algorithm for de novo circular RNA identification, *Genome Biol.*, 16, 4.
61. Liu, Y.-C., Li, J.-R., Sun, C.-H., et al. 2015, CircNet: a database of circular RNAs derived from transcriptome sequencing data, *Nucleic Acids Res.*, 44, D209–15.
62. Capel, B., Swain, A., Nicolis, S., et al. Circular transcripts of the testis-determining gene *Sry* in adult mouse testis, *Cell*, 73, 1019–30.
63. Lu, T., Cui, L., Zhou, Y., et al. 2015, Transcriptome-wide investigation of circular RNAs in rice, *RNA*, 21, 2076–87.
64. Jeck, W. R. and Sharpless, N. E. 2014, Detecting and characterizing circular RNAs, *Nat. Biotech.*, 32, 453–61.

65. Laitinen, P. J., Brown, K. M., Piippo, K., et al. 2001, Mutations of the cardiac ryanodine receptor (RyR2) gene in familial polymorphic ventricular tachycardia, *Circulation*, **103**, 485–90.
66. Meredith, C., Herrmann, R., Parry, C., et al. Mutations in the slow skeletal muscle fiber myosin heavy chain gene (*MYH7*) cause late-onset distal myopathy (MPD1), *Am. J. Hum. Genet.*, **75**, 703–8.
67. Walsh, R., Rutland, C., Thomas, R. and Loughna, S. 2010, Cardiomyopathy: a systematic review of disease-causing mutations in myosin heavy chain 7 and their phenotypic manifestations, *Cardiology*, **115**, 49–60.
68. Schiaffino, S., Dyar, K. A., Ciciliot, S., Blaauw, B. and Sandri, M. 2013, Mechanisms regulating skeletal muscle growth and atrophy, *FEBS J.*, **280**, 4294–314.
69. González-Mariscal, L., Domínguez-Calderón, A., Raya-Sandino, A., Ortega-Olvera, J. M., Vargas-Sierra, O. and Martínez-Revollar, G. 2014, Tight junctions and the regulation of gene expression, *Semin. Cell Dev. Biol.*, **36**, 213–23.
70. González-Mariscal, L., Lechuga, S. and Garay, E. 2007, Role of tight junctions in cell proliferation and cancer, *Prog. Histochem. Cytochem.*, **42**, 1–57.
71. Salzman, J., Gawad, C., Wang, P. L., Lacayo, N. and Brown, P. O. 2012, Circular RNAs are the predominant transcript isoform from hundreds of human genes in diverse cell types. *PLoS One*, **7**, e30733.
72. Ghosal, S., Das, S., Sen, R., Basak, P. and Chakrabarti, J. 2013, Circ2Traits: a comprehensive database for circular RNA potentially associated with disease and traits, *Front. Genet.*, **4**, 283.
73. Zheng, L.-L., Li, J.-H., Wu, J., et al. 2016, deepBase v2.0: identification, expression, evolution and function of small RNAs, lncRNAs and circular RNAs from deep-sequencing data, *Nucleic Acids Res.*, **44**, D196–202.
74. Dudekula, D. B., Panda, A. C., Grammatikakis, I., De, S., Abdelmohsen, K. and Gorospe, M. 2015, CircInteractome: a web tool for exploring circular RNAs and their interacting proteins and microRNAs, *RNA Biol.*, **13**, 34–42.
75. Bhattacharya, A. and Cui, Y. 2016, SomamiR 2.0: a database of cancer somatic mutations altering microRNA–ceRNA interactions, *Nucleic Acids Res.*, **44**, D1005–10.